Project 094 Probabilistic Unmanned Aircraft System (UAS) Trajectory and Noise Estimation Tool

Georgia Institute of Technology

Project Lead Investigators

Prof. Dimitri N. Mavris
Director, Aerospace Systems Design Laboratory
School of Aerospace Engineering
Georgia Institute of Technology
Phone: (404) 894-1557
Fax: (404) 894-6596
Email: dimitri.mavris@ae.gatech.edu

Dr. Holger Pfaender
Aerospace Systems Design Laboratory
School of Aerospace Engineering
Georgia Institute of Technology
Phone: (404) 385-2786
Fax: (404) 894-6596
Email: holger.pfaender@ae.gatech.edu

University Participants

Georgia Institute of Technology (Georgia Tech)

- P.I.s: Dr. Dimitri N. Mavris (P.I.), Dr. Holger Pfaender (Co-P.I.)
- FAA Award Number: 13-C-AJFE-GIT-143
- Period of Performance: January 1, 2025, to December 31, 2025
- Tasks:
  1. Investigate and Implement Modeling Improvements
  2. Extend Sources of Uncertainty
  3. Extension to urban air mobility (UAM) operations
  4. Case Study Leveraging Previously Developed Methodologies
  5. Coordination with Federal Aviation Administration (FAA) and Volpe National Transportation Systems Center (Volpe)
  6. Documentation

Project Funding Level

The ASCENT Project 094 is funded by the FAA at the following levels: Georgia Tech ($335,000).

Georgia Tech has agreed to a total of $335,000 in matching funds. This total includes salaries for the project director, research engineers, and graduate research assistants and for computing, financial, and administrative support, including meeting arrangements. Georgia Tech has also agreed to provide tuition remission for students whose tuition is paid via state funds.

Investigation Team

Georgia Institute of Technology

Dimitri N. Mavris (P.I.)
Holger Pfaender (co-P.I.), Tasks 1-6
Raphaël Gautier (research faculty), Tasks 1-6
Jiacheng “Albert” Xie (research faculty), Tasks 1-6

Nada Himdi (graduate student), Tasks 1, 2, and 5
Venkat Sai Chinta (graduate student), Task 1
Zhiyao "Echo" Song (graduate student), Task 3
Kumanan Srinivasan (graduate student), Task 3
Lloyd Teta (graduate student), Tasks 1, 2, and 5
Xi Wang (graduate student), Task 3

Project Overview

Context and Motivation

The unmanned aircraft system (UAS) market is expected to grow rapidly in coming years, with projections estimating the civil UAS market at $121 billion in the next decade. Multiple operators are currently developing and testing various concepts of operations that fall within the umbrella of UAM, with the two main use cases being drone delivery and electric-vertical takeoff and landing (eVTOL) air taxis. Like traditional aircraft operations, these novel concepts are expected to have an impact on the environment in which they operate, particularly regarding noise. Just as noise assessments of traditional commercial and general aviation fixed wing and rotary aircraft operations are completed today, similar noise assessments for UAM operations will be necessary.

Problem Definition

UAM operations bring unique requirements. First, UAM operations are expected to be denser than current general or commercial aviation operations, possibly by orders of magnitude. Thus, a noise assessment method should be able to manage large vehicle densities. Second, UAM vehicles are expected to be smaller and therefore quieter (e.g., small drones for deliveries or helicopter-sized vehicles for eVTOL air taxis, benefiting from novel electric propulsion systems). As a result, the noise footprint of such vehicles is expected to be more localized. Therefore, noise exposure levels should be estimated with sufficient resolution. Third, instead of primarily following fixed trajectories dictated by approach and departure routes around airports, UAM vehicles are expected to operate point-to-point within populated areas. Departure and arrival locations are expected to vary from day to day; delivery drones may depart from warehouses and deliver goods to different customers every day, and eVTOL air taxis may allow their customers to be picked up and dropped off all around an urban area. Thus, a noise assessment method should be flexible enough to accommodate changing flight paths, and the resulting noise assessment should account for the variability introduced by these changes.

Research Objective

The objective of this research is to develop a novel noise estimation method/tool that supports the computation of noise resulting from the stochastic operation of UAS and other upcoming vehicle concepts with irregular locations and operations in large numbers.

Task 1 – Investigate and Implement Modeling Improvements

Georgia Institute of Technology

Objective

The objective of this task is to identify and implement improvements to the noise-modeling workflow that enhance both realism and computational efficiency. The work focuses on examining key components of the current modeling process, including input variability, operational assumptions, and data-handling methods, and introducing refinements that improve the accuracy and robustness of predicted noise exposure. This involves evaluating alternative statistical and computational techniques, streamlining the representation of operational data, and integrating modeling approaches that better capture the spatial and temporal characteristics of UAS and UAM activities. The overall goal is to produce a more efficient and reliable framework capable of generating consistent noise results across a wide range of operational conditions.

Research Approach

This section lays out the developed modeling and simulation framework and briefly discusses each step of the process. Representative results for each step are presented in the section devoted to Task 4, "Case Study Leveraging Previously Developed Methodologies."

Overview of Modeling and Simulation Framework

The overall workflow, illustrated in Figure 1, consists of four sequential stages that link operational modeling with noise assessment. The first two stages determine where flights may occur and how frequently they are expected, while the remaining stages evaluate their noise impact. In the first stage, feasible paths between staging locations and customers are identified using a path-planning algorithm that accounts for vehicle range, obstacles, and restricted airspace, yielding a set of potential flights with optimized routes. The second stage assigns each identified flight a probability based on spatial variations in demand and the presence of multiple operators. Using input noise source data, the third stage simulates single-event noise by converting planned paths into three-dimensional (3D) trajectories and propagating directional noise at each time step to obtain standard noise metrics. Finally, daily noise metrics are computed by selecting flights according to their assigned probabilities and aggregating their previously computed noise fields within a single day.

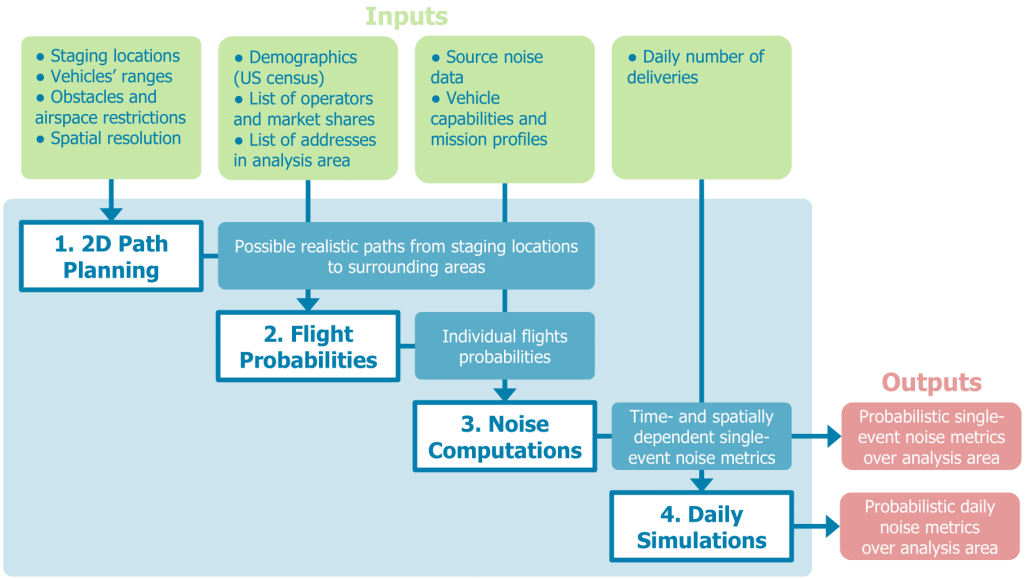

Figure 1. Refined workflow of drone delivery noise assessment.

Flight Path Planning

The first step of the workflow consists of identifying all feasible flights that may occur within the study area, given the locations of staging sites, vehicle range constraints, and the spatial distribution of customers. Straight-line navigation at a fixed altitude is insufficient in dense urban environments, where buildings, restricted airspace, and other obstacles must be avoided. A dedicated path-planning strategy is therefore required to produce realistic routes while maintaining computational efficiency. To balance these considerations, a two-step trajectory-generation process is employed: a two-dimensional track is first computed, and a fixed vertical profile is later applied when forming the full 3D trajectory for noise assessment.

Graph-based methods were identified as suitable due to their deterministic behavior and ease of implementation. The A⋆ algorithm (Hart et al., 1968) yields optimal grid-based paths but often produces pixelated trajectories unless smoothed. Its extension, Theta⋆ (Daniel et al., 2010), provides more realistic paths by allowing straight segments between non-adjacent cells when the line of sight is unobstructed, resulting in minor deviations from optimality that are acceptable for this application. Applying A⋆ or Theta⋆ to every origin–destination pair, however, becomes computationally prohibitive in large urban regions with hundreds of thousands of customer locations.

The adopted approach therefore relies on a modified Dijkstra algorithm (Dijkstra, 1959) augmented with Theta⋆-style line-of-sight checks implemented through a ray-tracing method (Amanatides & Woo, 1987). This formulation makes it possible to compute all reachable paths from each staging location in a single run, terminating once further cells would require exceeding vehicle range. The line-of-sight operation represents the dominant computational cost and is optimized using a Cython implementation. All feasible paths are stored in a database, enabling efficient retrieval of the appropriate two-dimensional track for any customer within range.

Flight Probability Calculation

Once all feasible flights and their corresponding paths are identified, the next step is to assign a probability to each of them so that the variability of drone delivery operations can be represented probabilistically. This requires estimating how likely each address is to place an order and then distributing this probability across the flights that can serve it.

Demand is treated in relative terms in order to capture how the likelihood of placing an order varies geographically. Since no dedicated drone-delivery demand model is available, the probability of online shopping is used as a proxy (Aller & Pahwa, 2020). The modeled shopping behavior using the multinomial logit formulation:

$$p(k|X) = \frac{e^{\beta_k X}}{1+\sum_{i=1}^{4} e^{\beta_i X}} \quad \text{(Eq. 1)}$$

where X represents demographic characteristics and k indexes four shopping categories: no shopping (k = 1), in-store shopping only (k = 2), online shopping only (k = 3), and both in-store and online shopping (k = 4). The probability of placing an online order is obtained by summing the two categories that involve online purchasing. Census demographic histograms are then used to aggregate these individual probabilities at the census-tract level:

$$p(o|a \in A_t) = \sum_{X \in C_t} \big(p(k=3|X) + p(k=4|X)\big) \times p(X) \quad \text{(Eq. 2)}$$

All addresses within tract t are assigned this same value. The resulting tract-level probabilities are normalized across all tracts so that the per-address probabilities sum to one:

$$p(a|o, a \in A_t) = \frac{p(o|a \in A_t)}{\sum_{\tau \in T} p(o|a \in A_\tau) \times \#(A_\tau)} \quad \text{(Eq. 3)}$$

After determining the order probability for each address, this value is subdivided among the flights capable of reaching the destination. If several operators can serve the address, the probability is divided among them using user-provided market shares, renormalized to include only operators with feasible paths. For a given operator, its share is further split among staging locations within range. A user-defined fraction is assigned to the closest staging location, and the remainder is evenly divided among the others.

The probability of an individual flight is the product of the address-level probability and the operator and staging-location components along its corresponding branch in the decomposition shown in Figure 2.

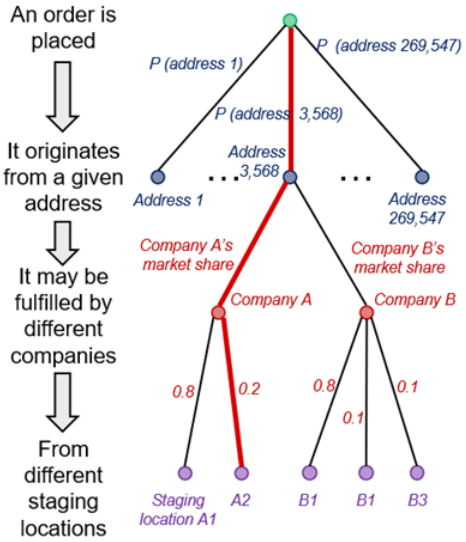

Figure 2. Tree diagram summarizing the process used to determine individual flights' probabilities.

Single-Event Simulation

1. Noise Propagation Model

The noise associated with each flight is evaluated using a propagation model consistent with the Society of Automotive Engineers' (SAE) ARP5534 standard (SAE, 2013). The 3D trajectory is first discretized in time, and the position of the vehicle at each timestep is mapped onto a rectilinear grid of virtual receivers covering the study area. A pre-processing procedure determines the maximum distance beyond which the propagated sound level is negligible. This allows the model to restrict computations to receivers located within the range of acoustic relevance.

At every timestep, the distance and 3D emission angles between the vehicle and each relevant receiver are calculated. These angles determine which element of the vehicle's directional noise sphere is selected for that position in the trajectory. The selected spectrum is propagated to the receiver on a frequency-band basis following the procedures defined in ARP5534, and the resulting band levels are combined using A-weighting to produce instantaneous sound pressure levels. The independence of individual flights enables the noise-propagation calculations to be executed in parallel.

2. UAS Noise Source Modeling

The noise source sphere is a required input for noise propagation using the ASCENT Project 094 tool. Previously, the tool utilized a single noise source sphere on all flight phases and flight conditions. This is not realistic for the drone delivery application which is sensitive to varying flight conditions.

In the following, we discuss the generation of four distinct noise source sphere data for different (a) flight phases, (b) weights, (c) speeds, and (d) altitudes.

The four considered flight phases are hover, takeoff, cruise, and landing. The altitude was categorized as low (~35 ft above ground level [AGL]), medium (~90 ft AGL), and high (200 ft AGL). For the weight, the maximum and empty weights are respectively considered to represent the drone with and without the payload.

Generating noise source data for UAS relies on three analysis tools. The first two are from Volpe: (1) the Advanced Acoustics Model (AAM) and (2) the Acoustic Repropagation Technique (ART). The third is an in-house sound sphere post-processing tool. The noise-sphere generation process is described thereafter.

Atmospheric conditions, microphone locations, and flight trajectories used in the Causey Airport measurements are first input into AAM. Using time- and geometric-based analyses, AAM calculates the propagation physics and geometric relationship between the noise source (UAS aircraft) and microphones. AAM then outputs a time-history file that includes the mapped relationship on a sphere for each trajectory point.

ART uses microphone measurement data, aircraft specifications, and the time-history file generated by AAM as inputs to generate the vehicle's noise source data. This noise sphere is obtained by applying the propagation corrections from AAM to the measured microphone spectral time histories. These histories are then mapped into a 3D spectral source description, stored as a NetCDF file. Figure 3 illustrates an example of a generated noise sphere visualized in Tecplot.®

® Tecplot is a registered trademark of Tecplot, Inc., Bellevue, Washington.

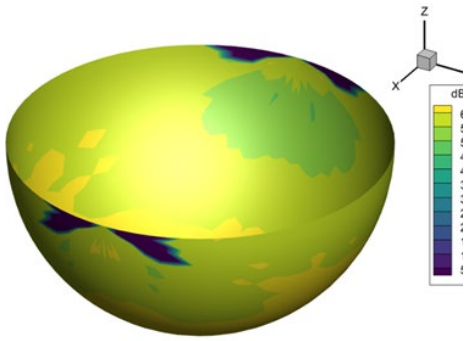

Figure 3. Example of a generated noise sphere.

3. Output Of Noise Propagation

The propagation model yields, for each flight, a time series of A-weighted sound levels at all receivers located within the propagation radius. These time histories reflect the directional source noise selected at each time step based on the vehicle's position, attitude, and flight phase. Integrating the received levels over the duration of the trajectory produces standard single-event noise metrics such as $L_{A,eq}$ and $L_{A,max}$. The complete set of receiver values forms the spatial noise footprint associated with that flight.

Probability-weighted results may also be constructed at the single-event level by combining the noise output of each flight with its previously computed flight probability. This enables the formation of probability distributions for single-event noise metrics across all feasible flights. These distributions characterize the variability in noise outcomes resulting from differences in routing, receiver geometry, and operational demand patterns.

Daily Simulation

The daily simulation models all delivery flights within a day to assess the overall noise exposure. Daily simulations are carried out by sampling flights according to their probability distribution. The total number of flights happening within a day is a user input, such that studies can be carried out for different envisioned daily volumes. Flights are then distributed within the day, and the results of the noise propagation step are leveraged, now accounting for the fact that the noise of multiple flights may be perceived by a virtual receiver at any given time step. The noise sources associated with the different vehicles are assumed to be uncorrelated, such that their noise energy can be summed. Alternate noise metrics, such as the day-night average sound level (DNL), can be computed from the outcome of daily simulations. The daily simulation is further discussed in additional detail in the section devoted to Task 2, "Extend Sources of Uncertainty."

Milestones

- Completed the workflow for path generation, flight-probability assignment, and single-event noise propagation.
- Integrated phase-specific noise spheres and ARP5534-based propagation into the ASCENT Project 094 tool.
- Validated distance/angle calculations and noise-sphere interpolation against AAM outputs.

Major Accomplishments

- Generated realistic obstacle-avoiding paths and assigned probabilities to all feasible flights.
- Implemented single-event noise simulation using directional noise spheres.
- Refined the model by adding reflected sound and adjusting propagation timing to improve agreement with AAM.

Plans for Next Period

- Introduce a step that precomputes noise for each flight phase and reuses it across time steps.
- Replace per-step propagation with fast lookups to reduce database size and improve runtime.

References

Aller, M., & Pahwa, A. (2020). Evaluating the environmental impacts of online shopping: A behavioral and transportation approach. *Transportation Research Part D: Transport and Environment, 80*. https://doi.org/10.1016/j.trd.2020.102223

Amanatides, J., & Woo, A. (1987). A fast voxel traversal algorithm for ray tracing. *Eurographics*, 3–10. https://doi.org/10.2312/EGTP.19871000

Center, V. (2020). *Advanced Acoustic Model (AAM) Technical Reference and User's Guide.* U.S. Department of Transportation.

Committee, A. R. (2024). *Census Data Manifest 2019–2023*. Atlanta Regional Commission. https://opendata.atlantaregional.com/pages/census-data-arc

Community, T. S. (2019). *scipy.spatial.distance.cdist — Reference Guide*. SciPy.org. https://docs.scipy.org/doc//scipy-1.3.2/reference/generated/scipy.spatial.distance.cdist.html

Community, T. S. (2023). *scipy.interpolate.interp1d — Manual*. SciPy.org. https://docs.scipy.org/doc/scipy/reference/generated/scipy.interpolate.interp1d.html

Daniel, K., Nash, A., Koenig, S., & Felner, A. (2010). Theta*: Any-angle path planning on grids. *Journal of Artificial Intelligence Research, 39*(1), 533–579.

Developers, S.-L. (2023). *Linear Models — User Guide*. Scikit Learn. https://scikit-learn.org/stable/modules/linear_model.html

Developers, S.-L. (2023). *Neural Network Models (Supervised) — User Guide*. Scikit Learn. https://scikit-learn.org/stable/modules/neural_networks_supervised.html

Dijkstra, E. W. (1959). A note on two problems in connexion with graphs. *Numerische Mathematik*, 1, 269–271. https://doi.org/10.1007/BF01386390

Hart, P. E., Nilsson, N. J., & Raphael, B. (1968). A formal basis for the heuristic determination of minimum cost paths. *IEEE Transactions on Systems Science and Cybernetics, 4*(2). https://doi.org/10.1109/TSSC.1968.300136

Heutschi, K., Ott, B., Nussbaumer, T., & Wellig, P. (2021). Virtual microphone signals of flying drones. *NATO STO MSG-SET-183 Specialists' Meeting on Drone Detectability* (pp. 27–29).

Hofferth, S., Flood, S. M., & Sobek, M. (2017). *American Time Use Survey Data Extract System: Version 2.6*. University of Maryland / University of Minnesota.

Jha, A. a. (2022). Urban Air Mobility: A preliminary case study for Chicago and Atlanta. *2022 IEEE/AIAA Transportation Electrification Conference and Electric Aircraft Technologies Symposium (ITEC+EATS)*, (pp. 300-306).

SAE. (2013). *Application of Pure-Tone Atmospheric Absorption Losses to One-Third Octave-Band Data (ARP5534).* SAE International.

Task 2 – Extend Sources of Uncertainty

Georgia Institute of Technology

Objectives

The objective of this task is to quantify uncertainty in the cumulative daily UAS noise exposure by incorporating variability in flight selection, scheduling, and service times. Current methods often analyze single flight events in isolation, which fails to capture the realistic noise environment where a receiver experiences multiple, overlapping events. Therefore, this research aims to develop a Monte Carlo simulation framework that models a full day of operations to produce probabilistic noise metrics, rather than deterministic point estimates.

Research Approach

During a typical day, a receiver location experiences multiple flight events due to outbounds and inbounds flight, potentially from different drones serving various customers and from different warehouses. To quantify the cumulative noise exposure from these concurrent events, a daily simulation model is required. This step utilizes the precomputed results from the previous stages: (1) a list of all possible flights identified, (2) their corresponding probability of occurrence for each path, and (3) the pre-computed time-series sound pressure level (SPL) noise footprints for every flight at every receiver. The overall daily simulation process is illustrated in Figure 4.

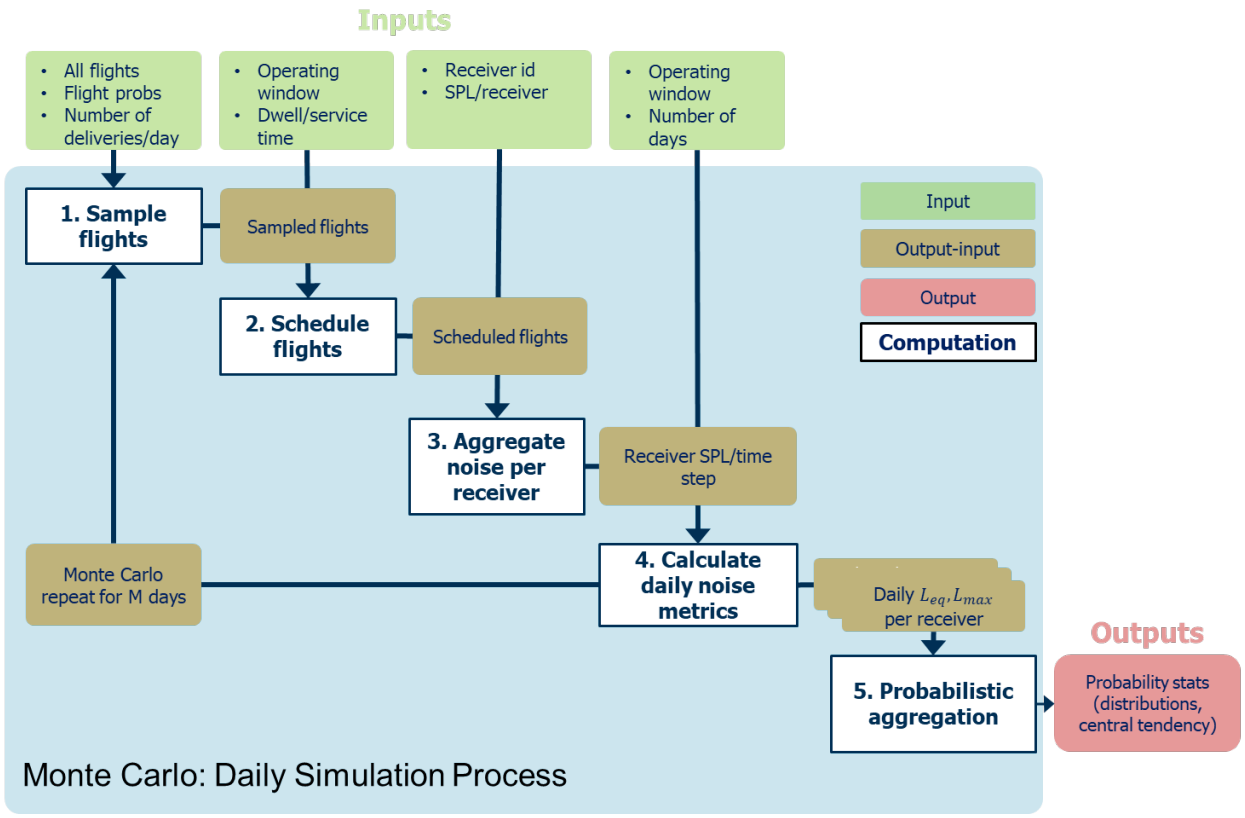

Figure 4. Implementation of the daily simulation process.

Single Day Simulation

The simulation process begins with the definition of the total number of flights occurring within a day, denoted as N. This parameter provides flexibility to analyze different daily operational volume scenarios. The computation of daily metrics follows a four-step process:

1. **Sample Flights:** The simulation samples N flights from the list of all possible paths. This sampling is weighted by each path's probability of occurrence. The draw is performed randomly with replacement to ensure that each sampled flight is independent and retains its original probability. The random sampling with replacement portrays the real world, demand driven characteristic of drone delivery operations where high-demand (high-probability) flight paths are likely to be used multiple times per day. That means high probability flights are likely to be sampled more than low probability flights.
2. **Schedule Flights:** Each of the N sampled flights is assigned a random departure time. These times are drawn from a uniform distribution over the defined operational window for the day, e.g., 8:00 a.m. to 10:00 p.m.
3. **Aggregate Noise:** Instead of recalculating noise propagation, the simulation leverages the pre-computed SPL time-series data. For a given receiver, the process accounts for the fact that noise from multiple flights may be perceived at any given time step. It offsets the SPL time-history of each sampled flight according to its random departure time. When flight events concurrently impact a specific receiver, the simulation aggregates the **acoustic energies** (a linear quantity) over the duration of the day to build a total, cumulative time-history of the noise footprint.
4. **Calculate Metrics:** From this aggregated daily time-history, the simulation calculates the primary daily noise metrics. These include (1) Maximum A-weighted Sound level, ($L_{max,day}$) which is the highest sound pressure level experienced at a particular time during the day and (2) Equivalent Continuous Sound Level ($L_{eq,day}$), which is the average exposure over operational window. Alternate metrics, such as DNL, time above threshold (TAT) can be computed from the outcome of daily simulations. This capability enables the exploration of metrics beyond peak loudness because a persistent drone presence may be more disturbing than a single loud flyover.

Monte Carlo Simulation

The daily simulation process described above is inherently stochastic. The output metrics $L_{max,day}$ and $L_{eq,day}$ are not fixed, deterministic values. They are the result of a system governed by random variables. There are two primary sources of this operational uncertainty:

1. **Path Selection Uncertainty:** It is unknown *which* of the thousands of possible flight paths will be used at any given time. The simulation models this by sampling flights based on their probability, to reflect day-to-day variability in customer demand.
2. **Scheduling Uncertainty:** It is unknown *when* each of those N flights will occur. The simulation models this by assigning random departure times within the operational window to mimic the unpredictable timing of individual orders.

The combination of these two factors creates a third, emergent source of uncertainty: *concurrency uncertainty*. On one simulated day, multiple flights may, by chance, have start times that cause their noise to overlap at a single receiver, leading to a high $L_{max,day}$. On another simulated day, those same flights might be spaced far apart, resulting in a lower $L_{max,day}$. Because the output is dependent on these random interactions, it is not possible to calculate a single, "correct" answer. The goal is to understand the *full range* of possible outcomes and their likelihood. This requires a method designed to solve problems using random sampling.

To address this stochastic system, this research employs the Monte Carlo simulation method. A Monte Carlo simulation is a computational technique that relies on repeated random sampling to obtain numerical results (Kissell, 2021). It is an ideal method for analyzing a complex system, like this one, where the interactions of random variables are too complex to be modeled by a simple equation. In this context, the four-step daily simulation process (sample, schedule, aggregate, calculate) is treated as a single "experiment" or "trial." The Monte Carlo simulation framework repeats this experiment M times, where M is a large, user-defined number of days. For each of the M iterations, a new set of N flights is sampled and a new set of random departure times are assigned. This mimics a new, unique, and plausible operational day of drone delivery.

Probabilistic Output

The final output of this M day simulation is a *probability distribution* for the daily noise metrics at each receiver. The simulation generates a list of M different $L_{max,day}$ and $L_{eq,day}$ values. The day-to-day variation of the daily metrics can be visualized as a histogram (an example is given in Figure 14 as part of the discussion of the notional results obtained for the Atlanta case study) and analyzed statistically to determine:

- The *mean* (the expected average exposure)
- The *median* (the 50th percentile, or "typical" day)
- The *95th percentile* (a "high noise" day, often used for policy and community impact assessment)

Milestones

- Completed initial implementation of the Monte Carlo simulation framework for daily noise analysis.
- Integrated pre-computed noise footprints (from Step 3) and flight probabilities (from Step 2) into the daily simulation environment.

Major Accomplishments

- Integrated flight sampling, random scheduling, and SPL aggregation into a repeatable simulation loop.
- Executed a preliminary large-scale test simulating 1000 operational days with 1,000 daily sampled flights per day.

Publications

None.

Outreach Efforts

None.

Awards

None.

Student Involvement
None.

Plans for Next Period
- Refine flight scheduling logic: Incorporate return flight and service/dwell times to increase operational realism.
- Improve computational efficiency through lookup SPL table caching and heading quantization to allow for large-scale simulations.
- Extend analysis from single point receivers to area wide spatial metrics (e.g., contour mapping) and new exposure metrics (e.g., time above threshold)

References
Kissell, R. L. (2021). Chapter 8 - Nonlinear Regression Models. In *Algorithmic Trading Methods* (2nd ed., pp. 197–219). Academic Press.

Task 3 – Extension to UAM Operations
Georgia Institute of Technology

Objectives
The objective of this task is to extend the current methodology to UAM operations. The preliminary phase is focused on defining a representative use case, specifically addressing the selection of a suitable location, identifying airspace constraints and the concept of operations.

Research Approach
Concept of Operation
UAM is rapidly transitioning from a futuristic concept to a near-term reality, propelled by technological advancements. Commercial UAM initiatives, ranging from conceptual design to full-scale flight-testing and active pursuit of regulatory certification, are maturing quickly. Companies have announced commercial plans for air taxi services on high-demand metropolitan routes (e.g., city centers to airports). Specifically, Archer Aviation plans airport shuttles and air mobility networks in the San Francisco Bay Area, Los Angeles, and New York. Wisk Aero® is targeting Houston, Los Angeles, and Miami. Joby Aviation® has announced plans for Los Angeles and New York.

On the academic side, many studies have been conducted to analyze UAM feasibility. A preliminary feasibility study for urban air mobility services in Chicago and Atlanta, by integrating eVTOL aircraft performance models (like the Joby® S4 and Lilium 7-seater) with a derived travel demand model based on commuter survey data was conducted (Jha, 2022). The analysis compares a potential UAM service against ground transportation, emphasizing that the viability and success of UAM hinges on meeting this projected travel demand by overcoming technical constraints, developing a necessary network of specialized infrastructure (vertiports), and achieving community acceptance to realize projected travel time reductions.

A study of the placement of UAM vertiports accounting for land use planning in the San Francisco Bay Area has also been conducted (Wei et al., 2023). It focuses on case studies in urban San Francisco, suburban San Jose, and exurban Livermore. The study establishes a systematic framework for vertiport site selection using a geographic information systems (GIS) suitability analysis. The core methodology employs a set of stakeholder-informed parameters categorized by safety, access, and equity, which are prioritized differently across the distinct geographic settings to determine site suitability. The goal is to provide planners with a replicable, cost-effective approach to identify suitable parcels and offer recommendations to integrate UAM network planning and land use regulations.

An analysis of optimal infrastructure placement for UAM air taxi services in New York City was conducted using a three-phased, data-driven approach (Senthilnathan et al., 2025). The research first uses the Clustering LARge Applications (CLARA) algorithm to identify a set of candidate vertiport and vertistop locations. Subsequently, an integrated genetic algorithm (GA)-simulation model is employed to select the most strategic final locations based on key operational metrics.

® Wisk Aero is a registered trademark of Wisk Aero, LLC, Mountain View, California.
® Joby and Joby Aviation are registered trademarks of Joby Aero, Inc., Santa Cruz, California.

These metrics prioritize factors such as minimizing rental cost, maximizing population coverage, ensuring favorable road facility access, and optimizing routing performance measures like customer waiting time, with the overarching goal of minimizing overall customer travel time within the air taxi system.

In addition to academic studies and industrial initiatives, work has also been done on the regulatory side. In the FAA's UAM Concept of Operations (Fontaine, 2023), a "crawl-walk-run" approach is outlined to operational maturation based on increasing tempo and complexity.

- Crawl Phase (Initial): New certified aircraft will operate under current regulatory frameworks and existing air traffic services (ATS) and routes, with the pilot in command onboard.
- Walk Phase (Intermediate): New regulations will accommodate a higher operational tempo, introducing UAM corridors that may not require traditional air traffic controller services, and allowing for preliminary remote pilot in command operations.
- Run Phase (Mature/Future): This high-tempo phase envisions new operational rules, a complex network of UAM corridors, and highly automated aircraft operating in a cooperative service environment called "extensible traffic management" (xTM).

The FAA's Advanced Air Mobility Implementation Plan targets achieving integrated AAM operations in the United States by 2028. Initial operations in the "crawl" phase are expected to be piloted and operated under the existing regulatory environment. Aircraft will fly under visual flight rules (VFR) using existing VFR constructs or specific chartered routes. Air traffic control (ATC) will provide services as needed, and operations will primarily use existing, modified airports and heliports.

Use Case Selection

To establish a consistent foundation for UAM demand modeling and vertiport network development, a comprehensive literature review was conducted across existing metropolitan use cases in New York, Chicago, Atlanta, and the San Francisco Bay Area. These prior studies provide insight into how bounding boxes are defined, how vertiport sites are selected, what vehicle types are assumed, and what methodological frameworks are used for demand estimation and infrastructure planning.

Based on the comparative assessment of these studies and considering regional airspace complexity, multimodal connectivity, zoning constraints, and the availability of high-quality operational data, the San Francisco Bay Area is selected as a representative use case due to its unique combination of dense urban development, complex airspace structure, and strong regional demand for high-capacity mobility solutions (see Table 1).

Table 1. Comparison of preceding studies on urban air mobility (UAM) network design for use case selection. ACS: American Community Survey, CLARA: Clustering LARge Applications, eVTOL: electric vertical take-off and landing, GIS: geographic information system, LODES: LEHD Origin-Destination Employment Statistics

City	Bounding area	Objective	Vertiport Selection	Vehicle Type	Technical Approach	Methodology Used
New York (NY)	Varied (high-density clusters)	Demand estimated using NY city taxi trip data, requiring ≥40% travel-time saving	Population density, access to transport, rental cost	Joby S4, Archer Midnight	Piloted eVTOL, high-density vertiport integration	CLARA Clustering, Genetic Algorithm (GA)
Chicago	50 mi × 50 mi	Derived from commute-time and congestion models using ACS LODES data	Commute time, income-based demand	Archer Midnight	Piloted eVTOL, infrastructure adaptation to helipads	GIS-based demand modeling, commute-time optimization
Atlanta	30 mi × 30 mi	Same as Chicago	Commute time, income-based demand	Joby S4, Wisk Cora	Mixed piloted + autonomous eVTOL models	GIS-based demand modeling, commute-time optimization
San Francisco (SF)	SF Bay Area	Multi-modal integration focusing on zoning and accessibility to transit	Land availability, zoning laws, demand clusters	Wisk Cora, Joby S4	Focus on autonomy (Wisk) and piloted ops (Joby)	GIS for vertiport site selection

Airspace Constraints

The San Francisco Bay Area contains one of the most complex and highly constrained terminal airspace environments in the United States. The region is shaped by the overlapping controlled airspace associated with San Francisco International Airport (KSFO), Oakland International Airport (KOAK), San Jose International Airport (KSJC), and numerous surrounding general-aviation airports. The KSFO Class B airspace imposes the highest level of control, requiring explicit ATC clearance and strict compliance with published transition instructions. The Class C airspace surrounding KOAK and KSJC requires two-way radio communication and transponder to always use. Although some outer segments may allow limited maneuvering, transitions generally follow established VFR procedures and ATC instructions. Several Class D airports, including Hayward (KHWD), Palo Alto (KPAO), and Reid-Hillview (KRHV), add additional altitude limits and localized traffic-pattern constraints. For modeling simplicity in this study, Class D regions are treated as uncontrolled airspace areas.

Guidance from the FAA's AAM Implementation Plan indicates that near-term eVTOL operations should rely on existing VFR and helicopter routes, while dedicated AAM corridors and special flight procedures are expected to emerge later. As a result, identifying workable transition procedures through Class B and Class C structures is a necessary step before generating feasible eVTOL flight paths. These airspace constraints directly affect allowable routing, transition altitudes, and the width of operational corridors throughout the Bay Area case study.

Transition procedures in the San Francisco Bay Area are derived by combining published VFR helicopter routes with data-driven analyses of historical flight-track patterns. Controlled airspaces around KSFO (Class B), KOAK (Class C), and KSJC (Class C) impose distinct altitude and lateral constraints that shape the feasible corridors for eVTOL operations. To identify representative transition paths, more than 40,000 piston-aircraft and helicopter tracks between 500 and 4000 ft mean sea level were clustered using the HDBSCAN algorithm (Campello et al., 2013). HDBSCAN is a clustering algorithm that identifies and separates groups of points or trajectories based on density, grouping flight paths where they naturally

concentrate and treating scattered or infrequent tracks as noise. Unlike parametric methods like K-Means, HDBSCAN identifies clusters without requiring a pre-specified number of groups. HDBSCAN improves traditional density-based methods by organizing data into a hierarchical structure, extracting clusters based on their stability over varying distance thresholds. All these features enable it to adapt to local variations in traffic density and capture clusters of arbitrary shape, making it effective for identifying the complex flight-track patterns found in congested airspace. Departure and arrival of trajectories were removed to isolate lateral transit behavior within each terminal area.

For the KSFO Class B inner circle, clustering reveals two primary transition patterns: (1) a San Francisco Bay Shore routing that follows the US-101 corridor and maintains separation from the 1,500–4,000 ft protected sectors and (2) a Pacific transition that remains offshore and merges eastbound near the coastline. In the KOAK Class C airspace, an outer "free fly" region exists north of the Bay Bridge below 3,000 ft, while the inner circle exhibits well-defined transitions, including the Coliseum routing and a Runway 30 parallel segment used to maintain lateral separation from airport operations.

Within the KSJC Class C inner circle, clustered tracks show a consistent mid-field crossing at approximately 2,000 ft and a fan-shaped set of pathways bounded by VPEMB, VPRPU, US-101, and I-680. These corridors aligned with helicopter practices and were further validated through consultations with local flight instructors. The resulting transition procedures provide structured, altitude-aware guidance for routing eVTOL trajectories through each controlled airspace while respecting existing ATC practices.

Validation against Aviation Environmental Design Tool

The objective of this subtask is to validate the in-house noise analysis tool (ASCENT Project 094 approach) using a National Aeronautics and Space Administration (NASA) UAM study conducted using the Aviation Environmental Design Tool (AEDT) (Rizzi & Rafaelof, 2023). Given the unique operational and acoustic characteristics of UAM vehicles, the study aims to overcome limitations in existing AEDT frameworks by generating noise-power-distance (NPD) data based on advanced simulation tools like NASA's Aircraft Noise Prediction Program (ANOPP2). The research focuses on segmenting point-to-point UAM operations into distinct departure, overflight, and approach phases, comparing noise exposure levels for fixed-wing, helicopter, and hybrid modeling approaches. The input data provided by the NASA UAM study group, along with the data generated by the AEDT, are utilized to replicate the study within the ASCENT Project 094 tool. This implementation serves as a critical component of the validation study, ensuring consistency and accuracy in noise modeling methodologies.

The validation process comprises two primary steps. The first step involves replicating the NASA UAM study within the AEDT, utilizing the input data provided by the NASA acoustics team. The output generated by the AEDT plays a crucial role in the second step of the validation process. In this step, the NASA UAM study is implemented within the ASCENT Project 094 tool, leveraging both the input data from NASA and the processed data from the AEDT. This phase requires extensive parsing and integration of multiple data files into the ASCENT Project 094 environment to ensure accurate and reliable implementation.

The discrepancies between AEDT and ASCENT Project 094 stem primarily from the fundamental differences in their noise modeling approaches, namely, AEDT's use of NPD curves versus ASCENT Project 094's use of noise spheres. Earlier observations from debug studies highlighted that AEDT's noise decay model behaves differently, particularly due to its method of computing slant range using the perpendicular distance from the closest point of approach. In contrast, ASCNET Project 094 applies the inverse square law, using the Euclidean distance between the source and the receiver at each time step. Further analyses revealed that AEDT's noise fraction adjustment introduces variability in the segment-wise contributions to the event-level sound exposure level (SEL). This adjustment was found to be highly sensitive to segment length, contributing to the uneven distribution of acoustic energy across the trajectory. Further differences arise from the treatment of source directivity: the AEDT uses lateral interpolation and extrapolation based on fixed azimuthal angles, producing broader, more diffuse contours, while ASCENT Project 094's full directivity model yields sharper, more localized noise regions. Across all analyses, a consistent trend was observed: ASCENT Project 094 tends to overpredict in takeoff and landing zones, while underpredicting during level flyover. However, the majority of undertrack deviations remain within 2–3 dBA, suggesting a reasonable level of agreement between the two tools under cruise conditions.

Milestones

- Conducted comprehensive review of academic literature and industrial plans regarding UAM deployment.
- Down selected the use case as the eVTOL transportation at the San Francisco Bay Area.

- Identified potential vertiport sites at the San Francisco Bay Area based on existing airports and preceding GIS-based UAM flight demand studies.
- Applied clustering algorithms to extract representative transition corridors from flight track data.
- Generated Origin-Destination pairs using performance-based mission-range criteria, producing a realistic set of eVTOL mission candidates.
- Formulated integrated obstacle zones, altitude bands, and transition areas for use in path-planning simulations.
- Implemented the NASA UAM case study within the ASCENT Project 094 tool, incorporating the input data, provided noise spheres and performance data reproduced from the original NASA acoustics study.
- Identified and analyzed discrepancies between ASCENT Project 094 and the AEDT, using diagnostic reports and detailed debug procedures to isolate sources of deviation between the two models.
- Performed an in-depth comparative assessment of the AEDT and ASCENT Project 094 noise propagation methodologies, outlining the key conceptual and computational differences that drive variation in their predictions.

Major Accomplishments

- Demonstrated a data-driven methodology for extracting operationally feasible transition paths from real flight-track data within constrained Class B and C airspaces.
- Integrated geometric airspace structures, local operating practices, and historical behavior into a unified transition-modeling framework.
- Established a reproducible workflow for mapping eVTOL routes that respect FAA-defined airspace layers and locally validated transition behaviors.
- Implemented and validated the NASA UAM case study within the ASCENT Project 094 tool.
- Completed a comprehensive diagnostic and comparative assessment of ASCENT Project 094 and the AEDT, identifying and examining the key sources of deviation.

Publications

None.

Outreach Efforts

None.

Awards

None.

Student Involvement

None.

Plans for Next Period

- Implement path planning algorithm to generate trajectories for use case study.
- Generate UAM travel demand for the designated study area.
- Generate altitude profiles and 3D trajectories for representative missions.
- Begin integration of noise-prediction workflows using trajectory outputs.
- Enhance the noise modeling capabilities in the ASCENT Project 094, with a particular focus on improving reflection and ground impedance modeling.

References

Wei, W., Rohrmeier, K., Martinez, T., Winans, M., & Park, H. (2023). *Land Use Analysis on Vertiports Based on a Case Study of the San Francisco Bay Area* (No. 23-13). San Jose State University. College of Business. Mineta Transportation Institute.

Senthilnathan, V. P., Singaravelu, M., Rajendran, S., & Srinivas, S. (2025). A clustering-metaheuristic-simulation approach to determine air taxi operating site location. *Transportation Research Interdisciplinary Perspectives*, 29, 101330.

Fontaine, P. (2023). Urban air mobility (UAM) concept of operations. Federal Aviation Administration, 800.

Campello, R. J., Moulavi, D., & Sander, J. (2013, April). Density-based clustering based on hierarchical density estimates. In *Pacific-Asia conference on knowledge discovery and data mining* (pp. 160-172). Berlin, Heidelberg: Springer Berlin Heidelberg.

Jha, A. a. (2022). Urban Air Mobility: A preliminary case study for Chicago and Atlanta. *2022 IEEE/AIAA Transportation Electrification Conference and Electric Aircraft Technologies Symposium (ITEC+EATS)*, (pp. 300-306).

Rizzi, S. A., & Rafaelof, M. (2023). On the modeling of UAM aircraft community noise in AEDT helicopter mode. *AIAA Aviation 2023 Forum.*

Task 4 – Case Study Leveraging Previously Developed Methodologies

Georgia Institute of Technology

Objectives

The Atlanta drone-delivery use case is introduced to illustrate the methodology developed in Task 1. This notional scenario provides a realistic urban context in which staging locations, customer addresses, and operational constraints are defined, allowing the full workflow—trajectory generation, demand-based probability estimation, and noise propagation setup—to be demonstrated on a representative environment. The results shown in the following sections reflect the application of this methodology to this specific test case.

Research Approach

Grid Definition

The notional setup is shown in Figure 5, where six staging locations are distributed between two operators (displayed in red and purple). The shaded discs represent nominal vehicle ranges of 5 km and 10 km. These discs provide only an approximate visualization of feasible operations, since obstacle avoidance is not yet considered and the true reachable areas will be smaller. The study area is defined as the union of these discs, expanded by a buffer chosen so that noise propagation is evaluated out to the distance where the maximum source level drops below a threshold of 30 dBA.

Once the study area is defined, residential addresses located within its boundaries are loaded, as illustrated in Figure 6. These addresses form the potential delivery destinations corresponding to the staging locations in Figure 6. The address distribution is non-uniform, and some regions contain few or no identifiable homes. This reflects limitations in the availability of public address data; because residential address lists are not openly released, data were manually collected through county offices. The spatial variability in address density influences the distribution of feasible flights and the resulting noise metrics.

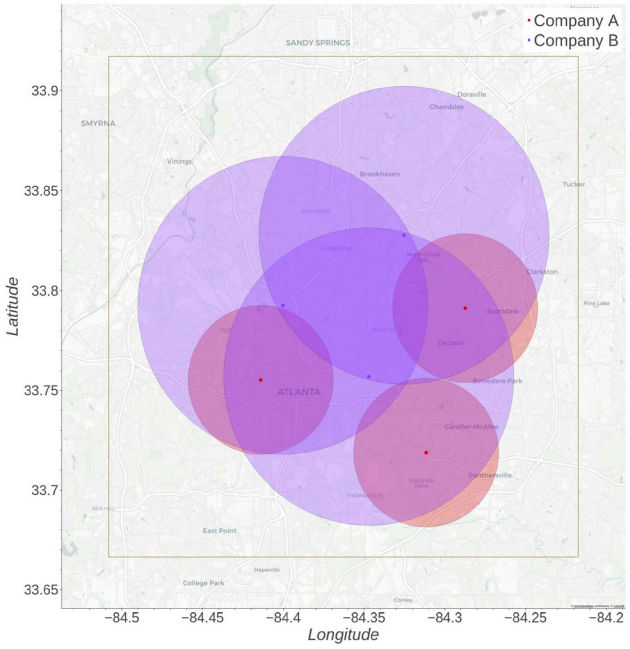

Figure 5. Map of the notional Atlanta use case showing six staging locations (red and purple).

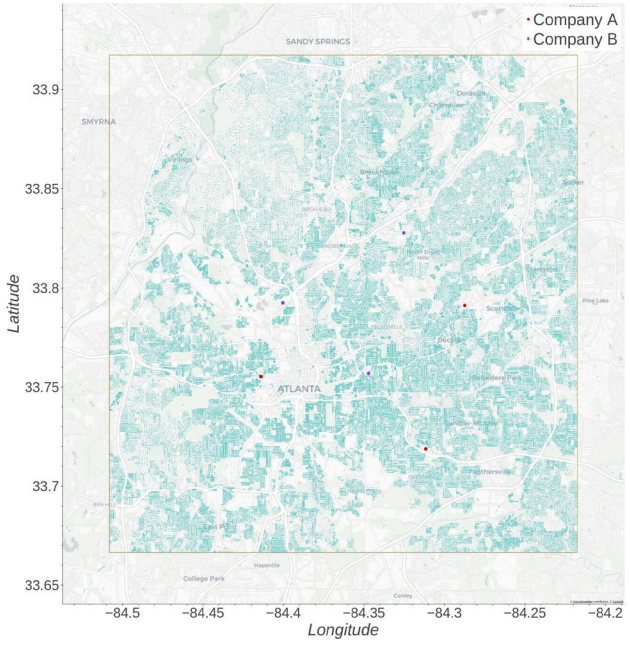

Figure 6. Scatter plot of the addresses loaded for the notional Atlanta use case.

Two-dimensional Flight Path Generation

The first stage generates paths between each staging location and the set of addresses while accounting for local obstacles. Two types of obstacles are included in this use case: (1) city parks, which some operators avoid, and (2) structures listed in the FAA obstacles database. These areas are rasterized onto the planning grid and treated as no-fly

regions. A subset of the resulting two-dimensional (2D) paths is shown in Figure 7, using colors corresponding to each operator. Only a limited sample of paths is displayed for clarity, as the full dataset includes roughly 300,000 destinations. Parks and FAA obstacles appear in green and dark blue, respectively, and the planned trajectories avoid both types of restricted areas. The modified Dijkstra-based routing method used here produces piecewise straight paths whenever unobstructed line-of-sight exists and remains computationally efficient. For example, computing all reachable paths for a single staging location with a 10 km range and a 50 ft grid resolution (about 430,000 cells) requires approximately 90 seconds on a laptop equipped with an Intel® Core i7-1370P processor. All computed paths are stored as waypoint sequences for use in subsequent steps.

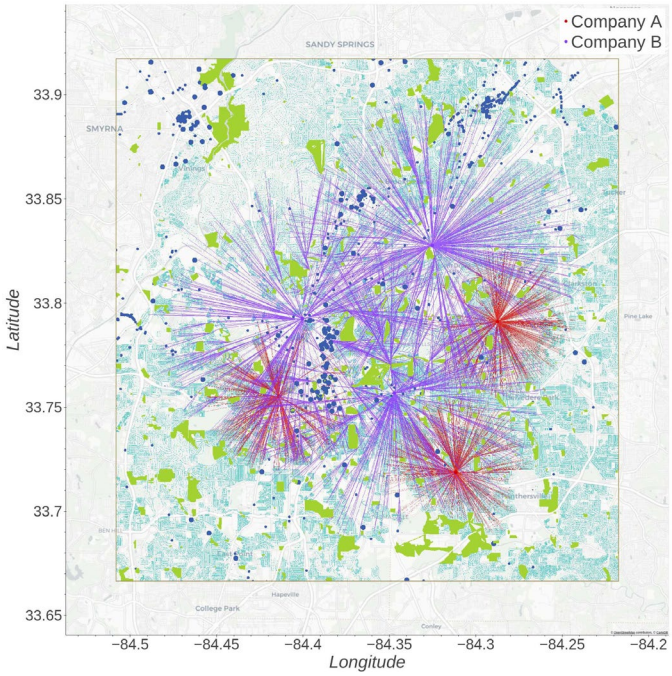

Figure 7. Subset of 2D tracks from the six staging locations to nearby customer addresses.

Flight Probability Calculation

After all feasible flights have been generated, the next step is to assign a probability to each flight. This is achieved by combining a spatial demand estimate with the operational reachability derived earlier. The address-level demand probabilities are shown in Figure 8, where each point is colored according to its estimated likelihood of placing an online order within a day. Since Census demographic information is defined at the tract level, all addresses within the same tract share the same probability value, producing the clearly delineated colored regions visible in Figure 8. These values are used only in a relative sense within the overall probability calculation.

Figure 9 highlights how many operators and staging locations can reach each address. Some addresses are served by only one staging location, while others fall within overlapping operational regions of one or more operators. These patterns reinforce the need for the hierarchical probability decomposition previously described, ensuring that the final flight probabilities reflect both demand distribution and operational accessibility.

® Intel is a registered trademark of the Intel Corporation, Santa Clara, California.

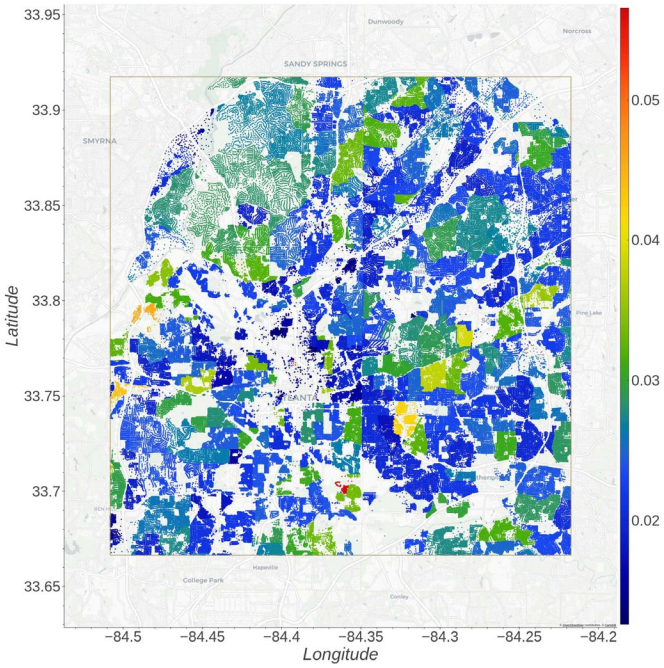

Figure 8. Scatter plot of addresses colored by daily order probability (lowest probabilities shown in blue, highest in red).

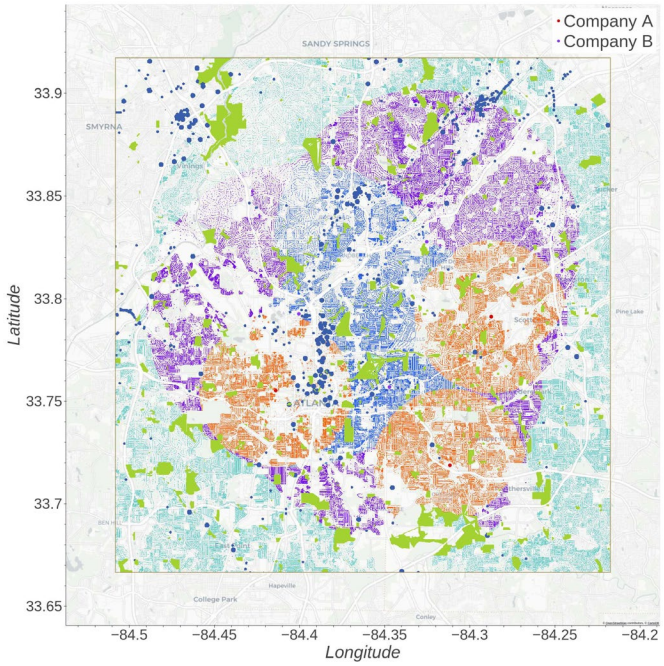

Figure 9. Scatter plot of addresses colored by how many companies and staging locations can serve them.

Single-Event Simulation Results

For a given flight, the stored 3D trajectory provides the vehicle's position at every timestep. Noise propagation is then carried out only to receivers lying within a 2 km radius of the path. These receivers correspond to the centers of the spatial grid cells. For each vehicle position, the distance and angular coordinates relative to each receiver are computed, and the appropriate noise sphere is selected based on the vehicle's instantaneous altitude and mission phase. Distinct noise spheres are used for the delivery leg (maximum weight) and for the return leg (empty weight), and phase transitions—such as climb, level flyover, or descent—are determined directly from altitude thresholds.

Taking the representative path shown in Figure 10 as an example, the receivers lying within the propagation radius are first identified. These receivers constitute the set to which source noise is propagated during the entire event. The resulting maximum A-weighted level, $L_{A,\max}$, is shown in Figure 11. This metric captures, for each receiver, the highest sound level experienced at any point along the flight. The contour clearly highlights the union of receivers contributing to the footprint, as well as the overall spatial extent of the event.

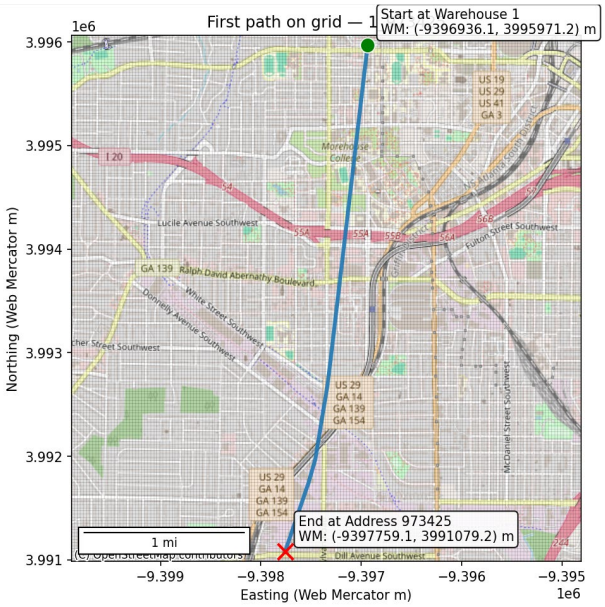

Figure 10. Selected two-dimensional path between a staging location and a customer address.

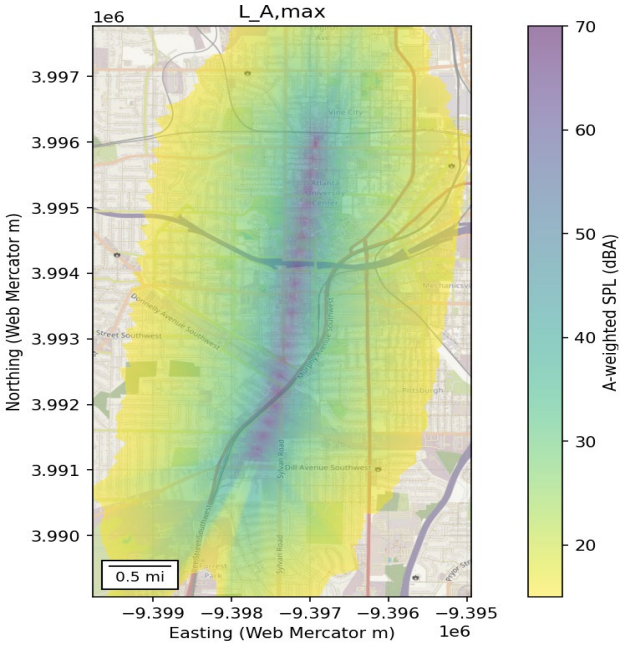

Figure 11. Single event, $L_{A,max}$, footprint of the selected two-dimensional path.

In addition to the $L_{A,\max}$ contour, it is also informative to examine the acoustic field at specific instants along the trajectory. Figure 12 and Figure 13 show the instantaneous A-weighted sound level for the delivery and return legs, respectively. In this example, the receivers located beneath the vehicle record approximately 61.7 dBA during the delivery leg and about 58.9 dBA during the return leg, reflecting the difference in vehicle mass. These instantaneous contours complement the $L_{A,\max}$ results by depicting the footprint at a particular moment during the flight.

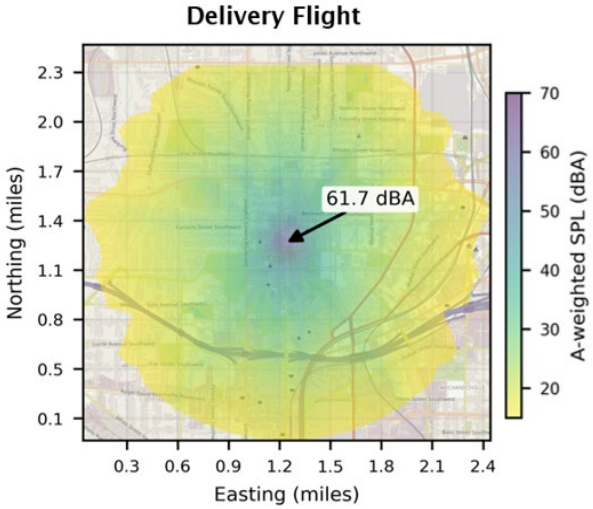

Figure 12. Instantaneous A-weighted sound pressure level (SPL) for the delivery leg.

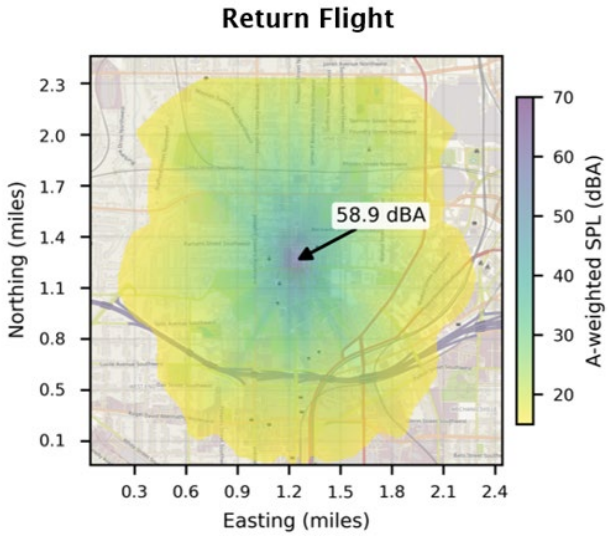

Figure 13. Instantaneous A-weighted sound pressure level (SPL) for the return leg.

Daily Simulation Results

The Monte Carlo is based on daily simulation that was implemented on a notional test case that has 1,877 candidate flights. Each simulated day samples 1,000 flights from this set based on their probabilities. The study repeats the daily simulation for 1,000 days. The simulation successfully generated probability distributions (histograms Figure 14) for both $L_{max,day}$ and $L_{eq,day}$.

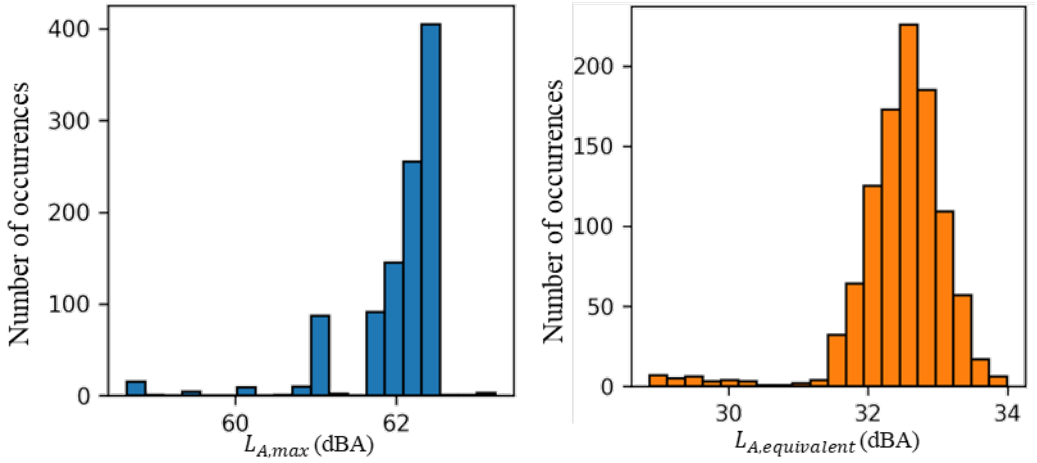

Figure 14. Notional results for a representative receiver.

As shown in the results for this receiver, this approach allows us to move beyond single-number estimates. Instead of one value, statistical measures like the mean and variance can be computed. The Monte Carlo simulation output provides a much richer understanding of the expected noise exposure and its variability, and this is essential for community noise assessment.

Milestones

- Established the Atlanta use case by defining staging locations, loading customer addresses, and initializing the study area for trajectory generation and noise analysis.

- Completed the full set of 2D flight paths for all feasible staging-location–to-address pairs and stored the resulting waypoint sequences for later noise propagation.
- Generated the complete set of flight probabilities using tract-level demand estimates and operator/staging-location reachability, producing probability values for every feasible flight.
- Verified the acoustic energy summation process to ensure accurate handling of overlapping flight events and correct conversion between linear energy and decibel metrics.

Major Accomplishments

- Established a simulation environment for UAS fleet operational noise assessment with demand model, flight trajectory optimization, and noise propagation integrated.
- Validated the noise computation module by comparing propagation results to AAM/ART using Causey UAS measurement data.
- Generated probabilistic distributions for $L_{eq,day}$ and $L_{max,day}$ metrics to quantify daily noise variability.

Publications

None.

Outreach Efforts

None.

Awards

None.

Student Involvement

None.

Plans for Next Period

- Reduce computational and storage demands for the single-event simulation database created for daily simulations for the UAS task.
- Visualize uncertainty and spatial distribution with contour maps for the UAS community noise exposure metrics.